LA-UR -86-279

Received by OSTI

SEP 0 8 1986

CONF-8608111--1

Los Alamos National Laboratory is operated by the University of California for the United States Department of Energy under contract W-7405-ENG-36.

LA-UR--86-2791

DE86 015327

TITLE: **MASSIVE SULFIDE DEPOSITS AND HYDROTHERMAL SOLUTIONS: INCREMENTAL REACTION MODELING OF MINERAL PRECIPITATION AND SULFUR ISOTOPIC EVOLUTION**

AUTHOR(S): David R. Janecky

SUBMITTED TO: To be presented at the Seventh Quadrennial IAGOD Symposium, Lulea, Sweden, August 17-22, 1986
(To be published in the Proceedings of the Seventh Quadrennial IAGOD Symposium, Lulea, Sweden, August 17-22, 1986)

DISCLAIMER

This report was prepared as an account of work sponsored by an agency of the United States Government. Neither the United States Government nor any agency thereof, nor any of their employees, makes any warranty, express or implied, or assumes any legal liability or responsibility for the accuracy, completeness, or usefulness of any information, apparatus, product, or process disclosed, or represents that its use would not infringe privately owned rights. Reference herein to any specific commercial product, process, or service by trade name, trademark, manufacturer, or otherwise does not necessarily constitute or imply its endorsement, recommendation, or favoring by the United States Government or any agency thereof. The views and opinions of authors expressed herein do not necessarily state or reflect those of the United States Government or any agency thereof.

By acceptance of this article, the publisher recognizes that the U.S. Government retains a nonexclusive, royalty-free license to publish or reproduce the published form of this contribution, or to allow others to do so, for U.S. Government purposes.

The Los Alamos National Laboratory requests that the publisher identify this article as work performed under the auspices of the U.S. Department of Energy.

Los Alamos

Los Alamos National Laboratory
Los Alamos, New Mexico 87545

MASTER

DISTRIBUTION OF THIS DOCUMENT IS UNLIMITED

DISCLAIMER

Massive sulfide deposits and hydrothermal solutions: Incremental reaction modeling of mineral precipitation and sulfur isotopic evolution

D. R. Janecky

Los Alamos National Laboratory, Los Alamos, NM 87545 (USA)

with 4 figures

Abstract: Incremental reaction path modeling of chemical and sulfur isotopic reactions occurring in active hydrothermal vents on the seafloor, in combination with chemical and petrographic data from sulfide samples from the seafloor and massive sulfide ore deposits, allows a detailed examination of the processes involved. This paper presents theoretical models of reactions of two types: (1) adiabatic mixing between hydrothermal solution and seawater, and (2) reaction of hydrothermal solution with sulfide deposit materials. In addition, reaction of hydrothermal solution with sulfide deposit minerals and basalt in feeder zones is discussed.

Active hydrothermal vents depositing sulfide structures on the seafloor provide a unique view of the dynamic processes involved during precipitation of seafloor massive sulfide deposits. Comprehensive characterization of the components of these systems has been provided by detailed investigation of hydrothermal solution composition, precipitated mineral assemblages, and precipitated mineral chemical and sulfur isotopic compositions from active hydrothermal vents on the seafloor (Von Damm *et al.*, 1985; Michard *et al.*, 1984; Haymon, 1983; Oudin, 1983; and therein), in combination with information from massive sulfide ore deposits (Franklin *et al.*, 1981; Ohmoto *et al.*, 1983; Sawkins, 1984; and references therein).

The primary process observed in active high temperature vents is mixing between hydrothermal solution and seawater (Figure 1). Massive sulfide ore deposits and active chimney samples, however, exhibit several features which can be ascribed to more complex pathways than simple mixing between hydrothermal solution and seawater (Figure 1), including Cu and Zn zoning of deposits, variable bulk sulfur isotopic compositions within districts (or samples), decreasing trends in sulfur isotopic composition upwards, and zones of wall-rock alteration and sulfide veins below the massive sulfide lenses, (Franklin *et al.*, 1981, Ohmoto *et al.*, 1983; Sawkins, 1984; Haymon, 1983; and references therein). Reactions within the seafloor and sulfide deposits associated with active venting must also be important, but are more difficult to identify. For example, Ca and Sr solution composition data indicate differences between vents or vent fields which are difficult to ascribe to water-rock reactions at the source of the hydrothermal solutions and may be due to dissolution of anhydrite within the growing massive sulfide deposit (Seyfried and Janecky, 1985). Similarly, variation in sulfide sulfur isotopic composition of solution samples with respect to time imply more complex processes (Shanks, unpublished data; Janecky and Shanks, in prep).

Incremental reaction path modeling allows examination of chemical processes during formation of massive sulfide deposits, including mineral precipitation, solution composition evolution and variability, and sulfur isotopic distribution. Two types of reactions have been modeled to examine formation of massive sulfide deposits and their features. These are (1) mixing between hydrothermal solution and seawater, either approximately adiabatically or with conductive heating or cooling, and (2) reaction

for Proceedings of the Seventh Quadrennial IAGOD Symposium, Luleå, Sweden 1986

of hydrothermal solution with previously precipitated sulfide/sulfate mineral products (Figure 1). An additional type of reaction (3) which has not been modeled, but will be discussed briefly involves interaction between hydrothermal solution and basalt wall-rock below the seafloor interface and formation of stockwork zones (Figure 1). Involvement of seawater (4) in the latter two types of reactions must be variable and, although important to our understanding of these processes, remains difficult to identify and quantify.

Reaction path modeling codes and data sets

Chemical reaction pathways have been calculated using the EQ3/6 reaction pathway modeling codes (Wolery, 1978, 1979, 1983). Dissociation constants for aqueous species used in this work were from the 250 bar data base of Janecky and Seyfried (1983), Janecky (1982), and Janecky and Seyfried (1984). Mineral dissolution constants, redox reaction constants, and gas fugacity relations were calculated using SUPCRT and data from Helgeson *et al.* (1978), Helgeson and Kirkham (1974a,b; 1976), Helgeson *et al.* (1981), and Helgeson (personal communication of updates and corrections to the data). Sulfate and sulfide aqueous species and minerals were treated either as being in total equilibrium, or as two separate sets of independent chemical components (see Janecky and Seyfried, 1984).

Sulfur isotopic distribution between solution components and sulfide minerals were calculated using the EQPS code (Janecky and Shanks, in prep) and data for sulfur isotopic fractionation factors from Ohmoto and Rye (1979). The EQPS code operates as a post processor to EQ6 and allows sulfur isotopic distribution to be calculated according to a variety of constraints, including: total isotopic equilibrium, sulfate-sulfide isotopic disequilibrium, and open or closed isotopic system where minerals may or may not continuously reequilibrate with solution as the reactions proceed. These isotopic constraints are selected in EQPS, independent of chemical equilibrium or disequilibrium constraints imposed during the EQ6 calculation.

Adiabatic mixing between hydrothermal solution and seawater

Calculation of the simple case of ˜350°C hydrothermal solutions mixing with ambient seawater approximately adiabatically, results in prediction of temperatures of mineral precipitation, paragenetic sequence of minerals, and chemical composition of the deposits consistent with active vent and massive sulfide ore deposits (Janecky and Seyfried, 1984). For the end-member case of total sulfate-sulfide chemical disequilibrium during mixing, the paragenetic sequence with respect to decreasing temperature of precipitation is: chalcopyrite, anhydrite, pyrrhotite, (pyrite,) sphalerite, (anhydrite dissolution), and barite (Figure 2a). When sulfate-sulfide equilibria is permitted during mixing, however, reduction of small amounts of sulfate results in early precipitation of pyrite and replacement of chalcopyrite with a sequence of Cu-rich sulfide minerals (bornite-chalcocite-covellite) as temperature decreases (Figure 2b). This latter sequence is analogous to that observed in thin chimney walls (Haymon, 1983), while the former is most typical of the chimneys and massive lenses as a whole. The calculations indicate that sulfide mineral precipitation occurs in response to both cooling and change in composition of the hydrothermal solutions as a result of mixing. Varying the amount of mixing with respect to decreasing temperature, simulating conductive heating of seawater prior to mixing or conductive cooling of the hydrothermal solution, results in only minor variations in the sequence and abundance of precipitated phases, particularly for sulfide minerals (Janecky and Seyfried, 1984; Janecky and Shanks, in prep). Quartz is super-saturated throughout the mixing process, but does not precipitate in most active vent systems and thus its precipitation was suppressed in these models. However, amorphous silica precipitates with sufficient conductive cooling of hydrothermal solution — at ~170°C for undiluted hydrothermal solution (Janecky and Seyfried, 1984).

Sulfur isotopic compositions have been calculated for models of hydrothermal solution mixing adiabatically with seawater, for both equilibrium and disequilibrium sulfate-sulfide reactions and a variety of isotopic constraints (Figure 3). Sulfate-sulfide chemical and isotopic disequilibrium, for an isotopically closed system, in general accurately models sulfur isotopic data for minerals from both active seafloor hydrothermal sulfide deposits and massive sulfide ore deposits (Figure 3a) (Shanks, unpublished data; Styrt *et al.*, 1981; Kerridge *et al.*, 1983; Zierenberg *et al.*, 1984; Franklin *et al.*, 1981 and references therein). However, sulfur isotopic compositions of dissolved H_2S (Kerridge *et al.*, 1983) are significantly higher than those calculated and not in equilibrium with associated chimney materials. Calculations for a sulfate-sulfide chemical equilibrium mixing reaction pathway (Figure 2b), under similar constraints as for Figure 3a, indicate that solution and sulfide mineral sulfur isotopic compositions can be increased by sulfate reduction associated with venting (Figure 3b). Thus, the solutions analyzed by Kerridge *et al.* (1983) may have been affected by sulfate reduction, while most sulfide minerals analyzed reflect previous precipitation of minerals from more pristine end-member hydrothermal solution. In contrast to the behavior of pyrite, chalcopyrite, and sphalerite, the decreasing $\delta^{34}S$ trend for bornite, chalcocite, and covellite inferred by these models is exactly the opposite of the compositional trends observed (Shanks, unpublished data). Formation of these latter three minerals, however, apparently involves secondary replacement of chalcopyrite in thin chimney walls (Haymon, 1983) and requires addition of sulfur and overall oxidation as illustrated in the following reaction:

$$\underset{\text{Chalcopyrite}}{CuFeS_2} + .4\,SO_4 + 1.2\,H_2 + .8\,H^+ = .2\,\underset{\text{Bornite}}{Cu_5FeS_4} + .8\,\underset{\text{Pyrite}}{FeS_2} + 1.6\,H_2O.$$

If reduction of sulfate goes to completion and the reduced sulfate is totally incorporated into the sulfide minerals, such a reaction will result in increases of approximately 3 ppt $\delta^{34}S$ of the Cu-bearing minerals, while insignificantly changing the pyrite composition. Such results are consistent with the data of Shanks (unpublished).

Hydrothermal solution reaction with sulfide deposit materials

The results above for sulfur isotopes indicate that reaction of previously formed anhydrite and sulfide minerals with hydrothermal end-member solution and/or seawater can change, through sulfate reduction, change the sulfur isotopic composition of sulfide in solution and precipitated minerals. In addition, such reactions may affect the amounts of metals carried by hydrothermal solutions as they vent to seawater and metal distributions within sulfide deposits. Petrographic investigations of active vent deposits are consistent with such reactions, indicating replacement of initial low to moderate temperature assemblages of anhydrite+pyrite+sphalerite by high temperature assemblages of pyrite+pyrrhotite+chalcopyrite±anhydrite±sphalerite as chimneys develop (Haymon, 1983; Haymon and Kastner, 1981; Styrt *et al.*, 1981; Oudin, 1983; Zierenberg *et al.*, 1984). Even very simple calculated reaction pathway models show that Zn in particular may be significantly increased in the high temperature solutions by reaction with massive sulfide materials (Figure 4a). Thus, such reactions can have a significant effect on the local bulk composition of sulfide materials (Figure 4b) and must be important in the development of large scale zoning of deposits from Cu rich cores to Zn rich margins (Franklin *et al.*, 1981; Ohmoto *et al.*, 1983). These models indicate that where sphalerite is absent, ophiolitic massive sulfide materials have reacted with hydrothermal solution at >275°C (Figure 2a) and a bulk solution to rock mass ratio >25 (Figure 4b). These calculations also indicate that only minor dissolution of anhydrite in necessary to saturate the hydrothermal solution, limiting the extent of sulfate reduction within the massive sulfide deposit and resulting shifts in mineral and solution sulfur isotopic compositions. Thus, the observation of generally decreasing bulk sulfur isotopic compositions upwards in massive sulfide ore deposits (Franklin *et al.*, 1981) may result from a combination of limited reducing potential of the hydrothermal solution and sulfide deposit and progressive exclusion of seawater as the deposit grows.

Hydrothermal solution reaction with basalt

Reactions between basalt and hydrothermal solution (±seawater) just below the seafloor in massive sulfide ore deposits are relatively obvious due to resulting alteration assemblages, have long been described, and their significance recognized (Franklin *et al.*, 1981; Ohmoto *et al.*, 1983; Sawkins, 1984; and references therein). The nature of the plumbing system near the seafloor may significantly influence the extent of such reactions, deposit characteristics, and venting solution composition. For example, highly distributed permeability within the hydrothermal flow zone can increase contact between solution and basalt, and thus reaction rates and extent, enhancing Fe, Na, and Ca metasomatism within the flow zone. Similarly, high permeability surrounding the hydrothermal flow zone could increase seawater ingres, allowing Mg metasomatism and sulfate reduction. Reaction of basalt minerals with hydrothermal solution resulting in Fe metasomatism may result in enhanced reducing potential of the solution as in the following reaction:

$$\underset{\text{Labradorite}}{Na_{.4}Ca_{.6}Al_{1.6}Si_{2.4}O_8} + 7.68\ Fe^{++} + 1.12\ SiO_{2(aq)} + 12.8\ H_2O$$

$$=$$

$$.64\ \underset{\text{Daphnite}}{Fe_{12}Al_{2.5}Si_{5.5}O_{20}(OH)_{16}} + .4\ Na^+ + .6\ Ca^{++} + 13.76\ H^+ + .8\ H_{2(aq)}$$

while reaction between seawater Mg and basalt results in significant chemical changes in rock composition, but little change in the composition of the resulting hydrothermal solution, as follows:

$$\underset{\text{Labradorite}}{Na_{.4}Ca_{.6}Al_{1.6}Si_{2.4}O_8} + 4\ Mg^{++} + 6.4\ H_2O$$

$$=$$

$$.4\ \underset{\text{Clinochlore}}{Mg_{10}Al_4Si_6O_{20}(OH)_{16}} + .4\ Na^+ + .6\ Ca^{++} + 6.4\ H^+$$

Reaction pathway models of the type discussed above may provide significant insight into the chemical processes occurring within stockwork zones, however, they will require further collection and integration of a variety of information, including relative mineral reaction rates and compositional changes for basalts and extent of involvement of previously precipitated sulfide products on local scales.

Acknowledgements: This work has benefited from discussion and collaboration with W. E. Seyfried, W. C. Shanks, T. S. Bowers, R. E. Haymon, J. R. Delaney, and R. E. McDuff, among others. Initial calculations were supported by NSF grants OCE-8315116, OCE-8400676, and OCE-8542276 to W. E. Seyfried, University of Minnesota. Preparation of this paper and continued refinement of these approaches to examining the consequences of water-rock interaction is supported by funding from USDOE Office of Basic Energy Science to Los Alamos National Laboratory.

References

Franklin, J. M., Lydon, J. W., and Sangster, D. F. (1981) Volcanic associated massive sulfide deposits. *Econ. Geol. 75th Anniv. Volume*, 485-627.

Haymon, R. M. (1983) Growth history of hydrothermal black smoker chimneys. *Nature* 301, 695–698.

Haymon, R. M. and Kastner, M. (1981) Hot spring deposits on the East Pacific Rise at 21°N: Preliminary description of mineralogy and genesis. *Earth Planet. Sci. Lett.* 53, 363–381.

Helgeson, H. C. and Kirkham, D. H. (1974a) Theoretical prediction of the thermodynamic behavior of aqueous electrolytes at high pressures and temperatures. I. Summary of the thermodynamic/electrostatic properties of the solvent. *Am. Jour. Sci.* 274, 1089-1198.

Helgeson, H. C. and Kirkham, D. H. (1974b) Theoretical prediction of the thermodynamic behavior of aqueous electrolytes at high pressures and temperatures. II. Debye-Huckel parameters for activity coefficients and relative partial molal properties. *Am. Jour. Sci.* 274, 1199-1261.

Helgeson, H. C. and Kirkham, D. H. (1976) Theoretical prediction of the thermodynamic behavior of aqueous electrolytes at high pressures and temperatures. III. Equation of state for aqueous species at infinite dilution. *Am. Jour. Sci.* 276, 97-240.

Helgeson, H. C., Kirkham, D. H., and Flowers, G. C. (1981) Theoretical prediction of the thermodynamic behavior of aqueous electrolytes at high pressures and temperatures. IV. calculation of activity coefficients, osmotic coefficients, and apparent molal and standard and relative partial molal properties to 600°C and 5 kb. *Am. Jour. Sci.* 281, 1249-1517.

Helgeson, H. C., Delany, J. M., Nesbitt, H. W., and Bird, D. K. (1978) Summary and critique of the thermodynamic properties of rock-forming minerals. *Am. Jour. Sci.* 278a, 229 p.

Janecky, D. R. (1982) Serpentinization of peridotite within the oceanic crust: Experimental and theoretical investigations of seawater-peridotite interaction at 200°C and 300°C, 500 bars. PhD. thesis, University of Minnesota. 244p.

Janecky, D. R. and Seyfried, W. E., Jr. (1983) The solubility of Magnesium Hydroxide Sulfate Hydrate in seawater at elevated temperatures and pressures. *Am. J. Sci.* 283, 831-860.

Janecky, D. R. and Seyfried, W. E., Jr. (1984) Formation of massive sulfide deposits on oceanic ridge crests: Incremental reaction models for mixing between hydrothermal solutions and seawater. *Geochim. Cos. Acta* 48, 2723–2738.

Janecky, D. R. and Shanks, W. C. (in prep) Seafloor massive sulfide deposits and hydrothermal solutions: Incremental reaction modeling and sulfur isotopic evolution of EPR and Juan de Fuca Rise systems.

Kerridge, J., Haymon, R. M., and Kastner, M. (1983) Sulfur isotope systematics at the 21°N site, East Pacific Rise. *Earth Planet. Sci. Lett.* 66, 91-100.

Michard, G., Albarede, F., Michard, A., Minster, J.-F., Charlou, J.-L., and Tan, N. (1984) Chemistry of solutions from the 13°N East Pacific Rise site. *Earth Planet Sci. Lett.* 67, 297-308.

Ohmoto, H., Mizukami, M., Drummond, S. E., Eldridge, C. S., Pisutha-Arnond, V., and Lenagh, T. C. (1983) Chemical processes of Kuroko formation. In *Econ. Geol. Monograph* 5, (eds. H. Ohmoto and B. J. Skinner), pp. 570–604.

Ohmoto, H. and Rye, R. O. (1979) Isotopes of sulfur and carbon. In *Geochemistry of hydrothermal ore deposits*, (ed. H. L. Barnes), pp 509–567.

Oudin, E. (1983) Hydrothermal sulfide deposits of the East Pacific Rise (21°N) Part I: Descriptive mineralogy. *Marine Mining* 4, 39-72.

Sawkins, F. J. (1984) *Metal deposits in relation to plate tectonics*, Springer-Verlag, Berlin Heidelberg, 325p.

Seyfried, W. E., Jr. and Janecky, D. R. (1985) Sr and Ca exchange during hydrothermal alteration of basalt/diabase. *EOS, Am. Geophys. Union* 66, 929.

Styrt, M. M., Brackmann, A. J., Holland, H. D., Clark, B. C., Pisutha-Arnond, V., Eldridge, C. S., and Ohmoto, H. (1981) The mineralogy and the isotopic composition of sulfur in hydrothermal sulfide/sulfate deposits on the East Pacific Rise, 21°N latitude. *Earth Planet. Sci. Lett.* 53, 382–390.

Tivey, M. A. and Johnson, H. P. (1985) A near-bottom magnetic survey over an active hydrothermal vent field: Northern Juan de Fuca Ridge. *EOS, Am. Geophys. Union* 66, 925.

Von Damm, K. L., Edmond, J. M., Grant, B., and Measures, C. I. (1985) Chemistry of submarine hydrothermal solutions at 21°N, East Pacific Rise. *Geochim. Cos. Acta* 49, 2197–2220.

Wolery, T. J. (1978) Some chemical aspects of hydrothermal processes at mid-oceanic ridges — a theoretical study I. — basalt-seawater reaction and chemical cycling between the oceanic crust and the oceans. II. — calculation of chemical equilibrium between aqueous solutions and minerals. Unpublished PhD. Thesis, Northwestern University.

Wolery, T. J. (1979) calculation of chemical equilibrium between aqueous solution and minerals: the EQ3/6 software package. UCRL-52658, Lawrence Livermore National Laboratory, Livermore, Ca.

Wolery, T. J. (1983) EQ3NR: *A computer program for geochemical aqueous speciation-solubility calculations: User's guide and documentation.* UCRL-53414, Lawrence Livermore National Laboratory, Livermore, Ca.

Zierenberg, R., Shanks, W. C., and Bischoff, J. (1984) Massive sulfide deposits at 21°N, EPR: Chemical composition, stable isotopes, and phase equilibria. *Geol. Soc. America Bull.* 95.

Figure Captions

Figure 1. Diagram of a hypothetical massive sulfide deposit in a fault zone showing locations of dynamic chemical reaction processes involving hydrothermal solution reaction with (1) seawater. (2) sulfide deposit minerals. and (3) basalt±sulfide minerals. Seawater addition to the latter two processes is also possible (4).

Figure 2. Mineral precipitate amounts and distribution relative to temperature for approximately adiabatic mixing reactions between 1 kg of 21°N. EPR. hydrothermal solution and ambient seawater (after Janecky and Seyfried. 1984). representative of process (1) in Figure 1. For the sulfate-sulfide chemical disequilibrium model (a). precipitation of pyrite and silicate phases was suppressed and stability of sphalerite calculated for various Fe contents with and without (shaded area) pyrrhotite precipitation. For the sulfate-sulfide chemical equilibrium model (b). only precipitation of silicate phases was suppressed.

Figure 3. Sulfur isotopic composition pathways for 1 kg of 21°N. EPR. hydrothermal solution (initial δ^{34}S of 1 ppt) mixing with seawater (δ^{34}S of 20 ppt) (Figure 2). The models were calculated assuming an open isotopic system and sulfate-sulfide isotopic disequilibrium for pathways corresponding to (a) the sulfate-sulfide chemical disequilibrium mixing pathway with pyrrhotite present (Figure 2a). and (b) the sulfate-sulfide chemical equilibrium mixing pathway (Figure 2b). In the latter case. seawater sulfate contributed to the sulfide isotopic composition only as it was chemically reduced.

Figure 4. Calculated isothermal reaction pathway of 0.73 Kg of bulk chimney materials (Figure 2a and Janecky and Seyfried. 1984) with 1 kg of hydrothermal solution for (a) solution composition of selected metals. sulfide. and f_{O_2}. (b) mineral assemblage. and (c) corresponding sulfur isotopic pathway using initial solution δ^{34}S of 1 ppt and mineral isotopic compositions from Figure 3a. In (b) and (c) saturated minerals and unsaturated reactant minerals are indicated by solid and dashed lines. respectively. The calculation was stopped when sphalerite saturated.

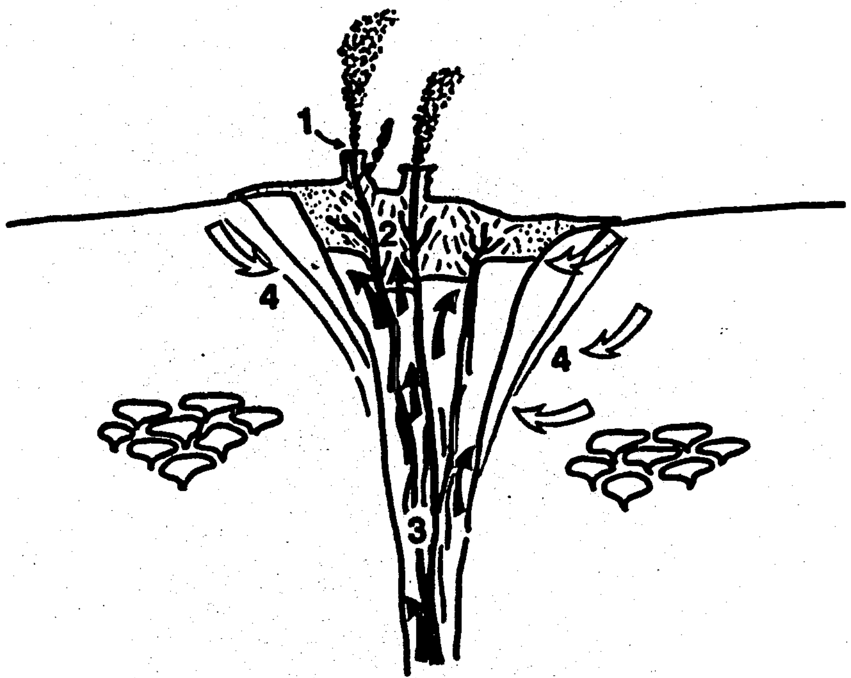
1
2
4
4
3

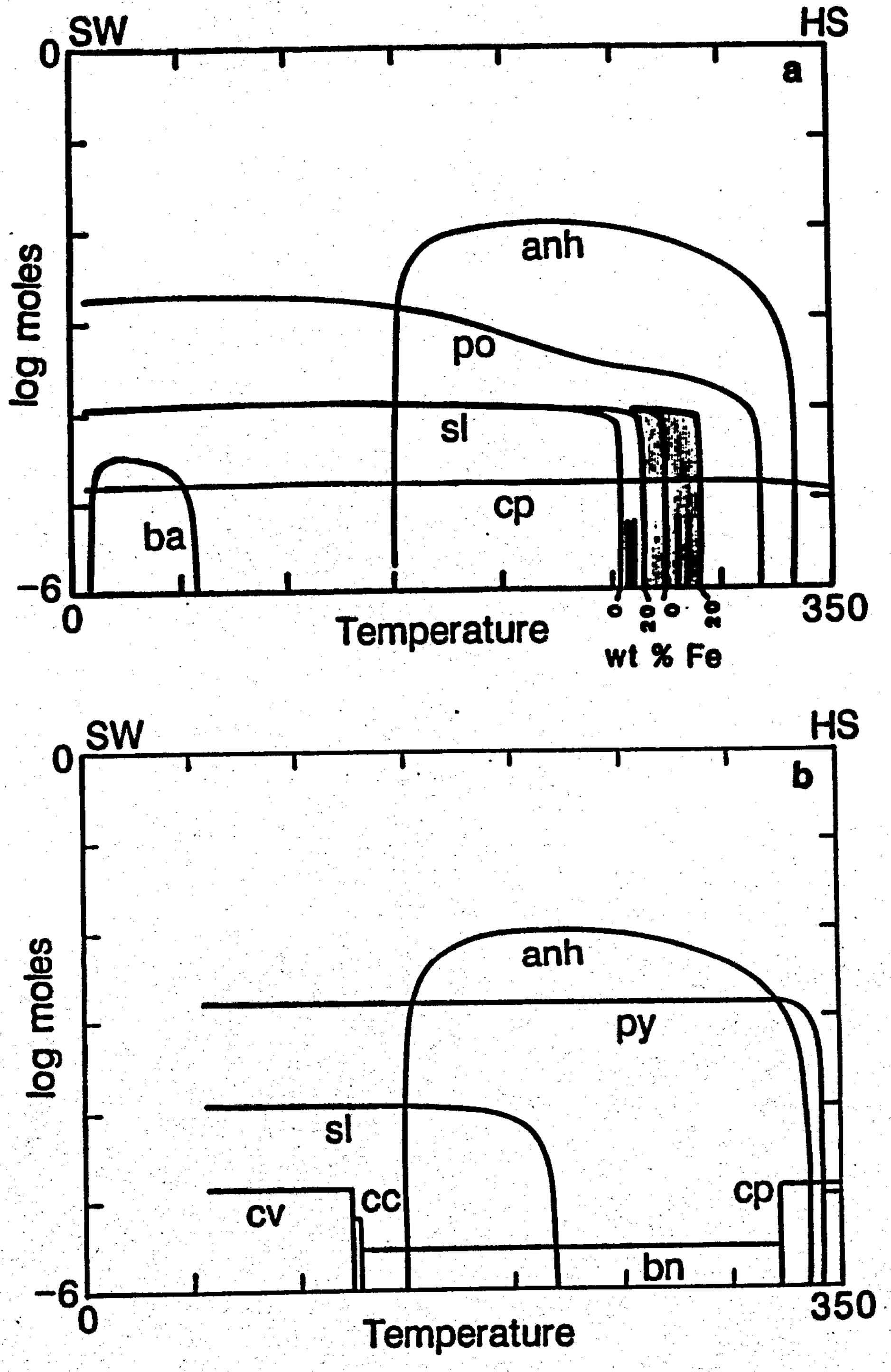
SW
HS
0
-6
a
log moles
anh
po
sl
cp
ba
0
350
Temperature
0
20
0
20
wt % Fe
SW
HS
0
-6
b
log moles
anh
py
sl
cv
cc
cp
bn
0
350
Temperature

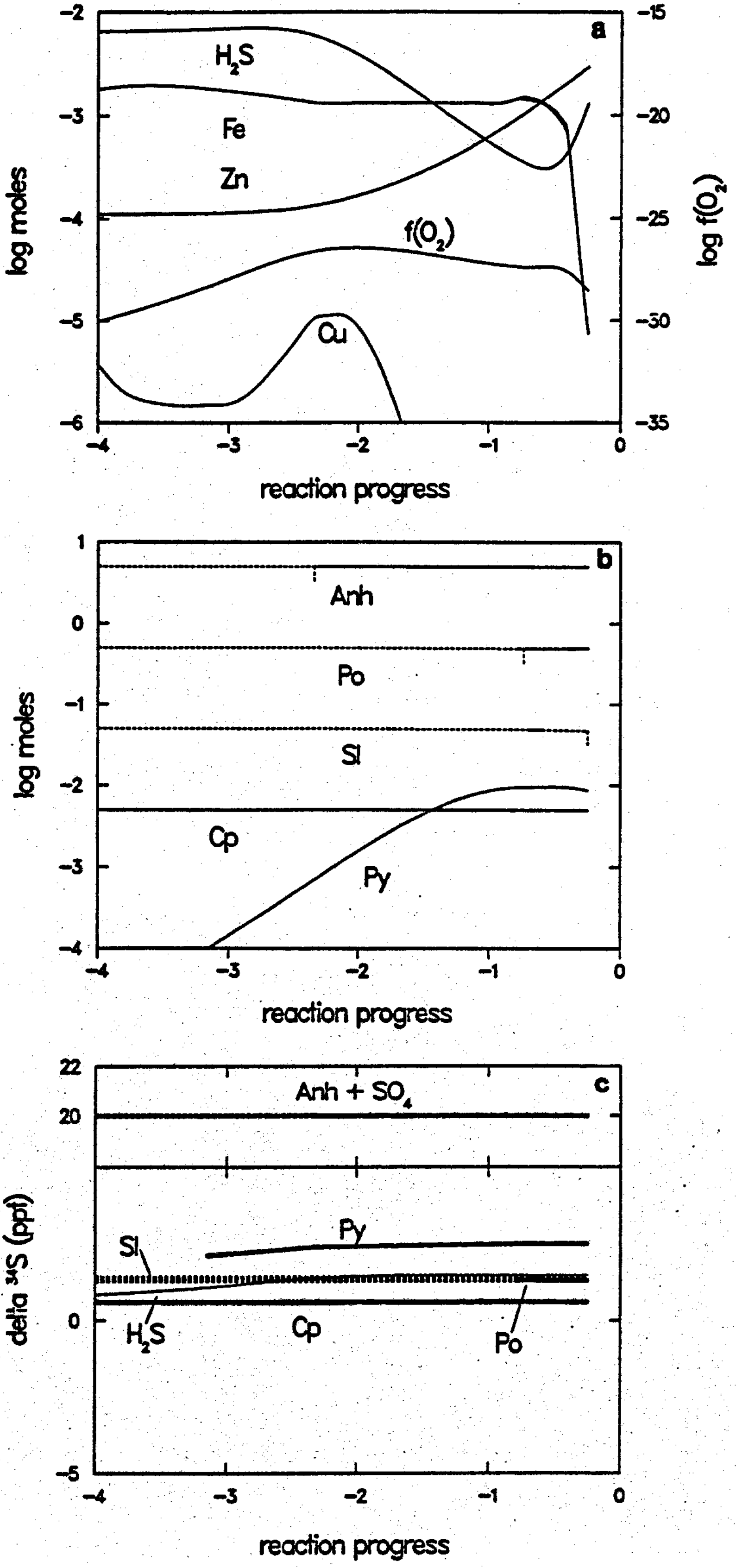
a
H$_2$S
Fe
Zn
f(O$_2$)
Cu
log moles
log f(O$_2$)
-2
-3
-4
-5
-6
-15
-20
-25
-30
-35
-4
-3
-2
-1
0
reaction progress
b
Anh
Po
Sl
Cp
Py
log moles
1
0
-1
-2
-3
-4
-4
-3
-2
-1
0
reaction progress
c
Anh + SO$_4$
Py
Sl
H$_2$S
Cp
Po
delta ^{34}S (ppt)
22
20
0
-5
-4
-3
-2
-1
0
reaction progress

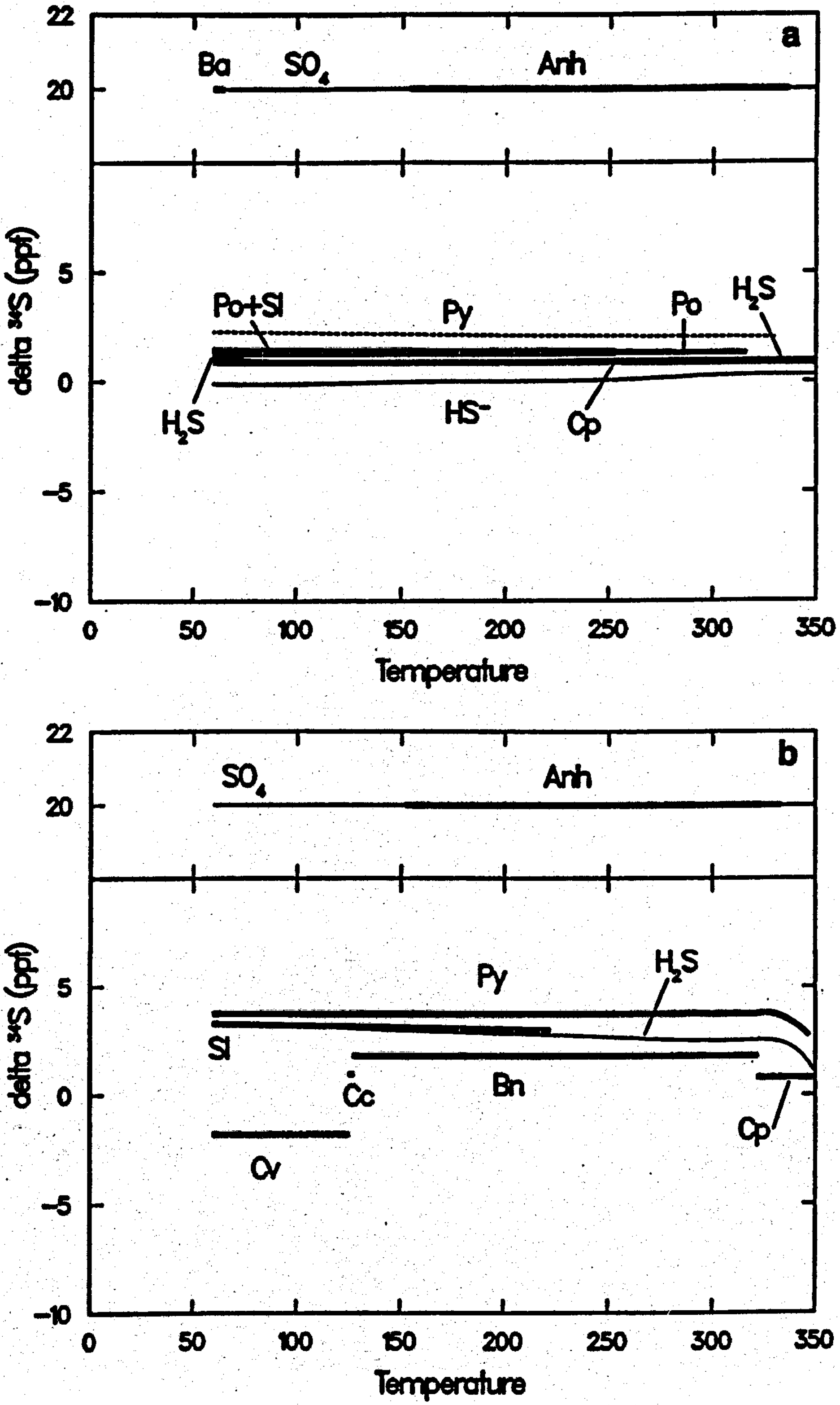
a
Ba
SO_4
Anh
Po+Sl
Py
Po
H_2S
H_2S
HS^-
Cp
delta ^{34}S (ppt)
22
20
5
0
−5
−10
0
50
100
150
200
250
300
350
Temperature
b
SO_4
Anh
Py
H_2S
Sl
Cc
Bn
Cp
Cv
delta ^{34}S (ppt)
22
20
5
0
−5
−10
0
50
100
150
200
250
300
350
Temperature